OPTOELECTRONICS AND ADVANCED MATERIALS – RAPID COMMUNICATIONS Vol. 7, No. 9-10, September - October 2013, p. 806 - 809

Ultrasonically assisted hydrothermal synthesis of nano-structured Bi_2Te_3 semiconductors for thermal energy recovery

P. SFIRLOAGA[a*], S. NOVACONI[a], P. VLAZAN[a], I. BADEA[a,b], I. GROZESCU[a,b]
[a]*National Institute for Research and Development in Electrochemistry and Condensed Matter, Timisoara, Condensed Matter Department, P. Andronescu Street, 300254, Timisoara, Romania*
[b]*"Politehnica" University from Timisoara, P-ta Victoriei Street, 34206, Timisoara, Romania*

Bismuth telluride semiconductors have been identified as potential high-performance thermoelectric materials, by offering an important thermoelectric-performance advantage for generating electrical energy from heat sources. Nanocrystalline powders of Bi_2Te_3 with different morphology and particle size 30-40 nm were prepared by ultrasonically assisted hydrothermal method of bismuth chloride and tellurium in aqueous solution with different concentration of $NaBH_4$ as reducing agent at 200°C for 5 hours and 80% fill degree of autoclave. The influences of precursors and hydrothermal treatment conditions on the formation features, phase composition, particle size, morphology and properties of the products were investigated by X-ray diffraction (XRD), scanning electron microscopy (SEM), energy dispersive spectroscopy (EDAX) and atomic force microscopy (AFM). The paper reports a comparative study regarding the precursors influence and hydrothermal condition of obtaining nano-structured thermoelectric materials. It was found that hydrothermal processing result in formation of low dimensional dispersion of Bi_2Te_3 nanostructures with desirable form and size and high degree of crystallinity.

(Received June 27, 2013; accepted September 18, 2013)

Keywords: Bismuth telluride, Thermoelectric materials, Hydrothermal method, Ultrasonic, semiconductors

1. Introduction

Thermoelectric (TE) materials are of interest for applications in solid-state cooling and electrical power generation devices due to many attractive features such as long life, no moving parts, no emissions of toxic gases, low maintenance, and high reliability [1, 2]. This are in generally a low cost materials that have a sufficiently strong thermoelectric effect (and other required properties), and could be used for applications including power generation, refrigeration and a variety of other applications. In the power generation case, thermoelectric devices convert the heat or in some case the waste heat into useful electricity [3]. Thermoelectric efficiency depends on the figure of merit, ZT There is no theoretical upper limit to Z and as Z approaches infinity, the thermoelectric efficiency approaches the Carnot limit. The figure of merit of a TE material is given by $Z = S^2\sigma/\kappa$, where S is the thermoelectric Seebeck coefficient, σ is the electric conductivity, and κ is the thermal conductivity of the material. A good TE material should have a high electrical conductivity and a low thermal conductivity. Bismuth telluride, Bi_2Te_3, and its compounds are most important TE materials used in state-of-the-art devices for the 200–400 K temperature range.

As a parent compound to many important thermoelectric semiconductor alloys, bismuth telluride (Bi_2Te_3) has been synthesized through different methods. Conventionally, it has been prepared through the metallurgical melt processing by mixing the appropriate amounts of the pure elements at elevated temperature of 500–600^{0}C [4, 5].

Many works have been done in the past years to improve their figure of merit by making the material nanostructured by doping this with different ions and making this materials with different shape like nanowire arrays [6,7] and quantum dot superlattice thin films [8,9]. For now, these materials are not suitable for large scale and economical TE applications, where bulk materials are used. In general a simple routine, like solvothermal routine are preferred to synthesize this materials [10, 11]. This method enables mass synthesis of materials with designed chemical compositions at a relative low temperature, and with little contamination on the material. There have been some reports of the synthesis of nanostructures Bi_2Te_3 based TE materials with solvothermal methods [12-16]. Also the hydrothermal route is used to synthesize nanostructures Bi_2Te_3 with different morphology [17]. Metal–organic chemical vapor deposition (MOCVD), in the III–V and II–VI semiconductors industry, was used to elaborate Bi_2Te_3 thin films [18-20].

We report obtaining of bismuth telluride nanostructures by ultrasonically assisted hydrothermal method and a comparative study regarding the precursors influence and hydrothermal condition on resulted materials. The influences of precursors and hydrothermal treatment conditions on the formation features, phase composition, particle size, morphology and properties of the products are also investigated by X-ray diffraction (XRD), scanning electron microscopy (SEM), energy dispersive spectroscopy (EDAX) and atomic force microscopy (AFM).

2. Experimental

Analytically pure chemicals (Aldrich) and pure tellurium 5N (Merch) were used for the synthesis of the sample in the present work. $BiCl_3$ and pure Te powder with Bi:Te mole ratio of 2:3 in aqueous solution with $NaBH_4$ as reductant and NaOH as pH regulator were used as the starting materials. This precursor was mixed and continuous stirred one hour for a better homogeneity and then was introduced in a Teflon lined steel autoclave with an immersed sonotrode [21]. The synthesis are made under a fill degree of autoclave about 80%, at pH 8,5 (S1) and 11 (S2) respectively, for 3 hour at 200°C under continuous ultrasonic at 200W and 40 KHz.

Sonication was performed using a power high voltage amplifier (connecting to computer via NI USB-6008 (National Instruments) equipped with an immersion ultrasonic sonotrode, which was made of titanium alloy, and with the tip diameter of 7 mm. The variable power output control allows the ultrasonic vibrations at the probe tip to be set to any desired amplitude and controlled by computer.

After the reaction, the autoclave was cooled to room temperature and then opened. The reaction product, a dark grey powder was filtered, washed with distilled water, ethanol and acetone several times, and dried to 60°C for 4 hours. More than 80% of the theoretical material amount was obtained after the drying.

Ultrasonic process was an important factor in this assisted hydrothermal synthesis of Bi_2Te_3 nanostructures. Firstly, reaction was generated by ultrasonation. When the reaction was performed without sonication, large quantity of unreacted tellurium remained in the product. Secondly, sonication was helpful to obtain relatively small and uniform particles.

The cavitation in liquid–solid systems produces mechano-chemical effects, in addition to the homogeneous cavitation observed in pure liquids. Liquid jets and/or shock waves formed under ultrasound irradiation can cause surface damage of the solid and/or produce high velocity interparticle collisions [21-23]. These effects, can produce particle breakage of Te, thus favored its dissolution and accelerated the reaction, and also can prevent the aggregation of the resulting nanocrystals. In addition, cavitation accelerates mass transport, and makes the repassivation by reaction products less important or even avoidable [24, 25].

In this ultrasonically assisted hydrothermal synthesis of Bi_2Te_3, the disproportionately of Te in alkaline solution (Eq. (1)) played a crucial role. Te^{2-} produced in the disproportionately of Te reacted with Bi (III) to give out Bi_2Te_3 (Eq. (3)). The mechanism may be as follows [26]:

$$3Te + 6OH^{-} \rightarrow 2Te^{2-} + TeO_3^{2-} + 3H_2O \qquad (1)$$

$$Bi(NO_3)_3 \rightarrow Bi^{3+} + 3NO_3^{-} \qquad (2)$$

$$2Bi^{3+} + 3Te^{2-} \rightarrow Bi_2Te_3 \qquad (3)$$

It was observed that the reaction speed increased along with the increment of NaOH, because more NaOH could drive Eq. (2) to move to the right side.

The phase structures of the prepared samples was investigated by X-ray diffraction (XRD) using PANalytical X'PertPRO MPD Difractometer with Cu *Kα* radiation λ = 1.5406Å, 2θ-step of 0.01◦ from 10 to 100. Scherrer equation, $d = 0.9\lambda/(B \cos \theta)$ was used to estimate grain average sizes of powders, where B is the half height width of the reflection peak at 2θ and λ is the wavelength of the radiation. Powder morphology was observed using an Inspect S PANalytical model scanning electron microscopy (SEM) and a NanoSurf atomic force microscopy (AFM). The semicantitative elemental analysis was analyzed through EDAX facility of SEM.

3. Results and discussions

3.1. XRD results

In Fig. 1 are presented the XRD patterns of different pH of bismuth telluride materials.

X-ray diffraction (XRD) analysis indicates that both hydrothermally synthesized samples have a single Bi_2Te_3 trigonal phase of R3m rhombohedral lattice structure. The average grain crystalites sizes estimated with Scherrer equation using the (0 1 5), (1 0 10) and (1 1 0) reflection are about 30 nm for S1 and about 40 nm for S2, respectively.

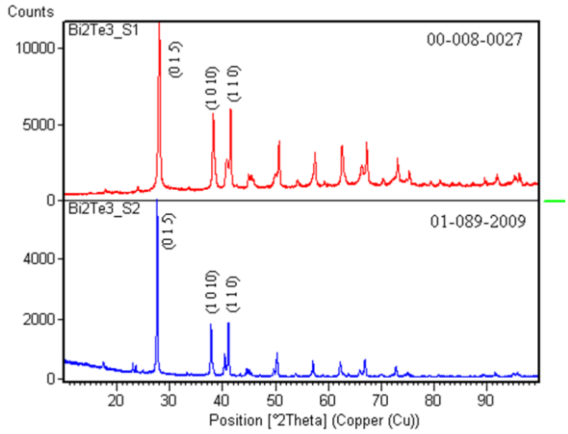

Fig. 1. XRD patterns of for Bi_2Te_3 synthesized by ultrasonically assisted hydrothermal method at 8.5 pH (S1) and 11 pH (S2).

3.2. SEM and EDX results

Figs. 2 and 3 represents the SEM images of the bismuth telluride synthesized by ultrasonic assisted hydrothermal method, at different pH values. The SEM morphology shows various topographies of the powders prepared by hydrothermal synthesis at different condition.

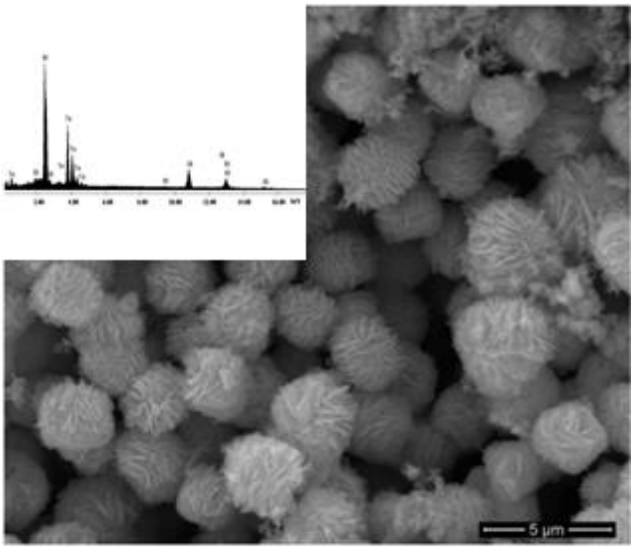

Fig. 2. SEM morphology for Bi_2Te_3 synthesized by ultrasonically assisted hydrothermal method at 8.5 pH; Inset: EDX spectra for elemental analysis.

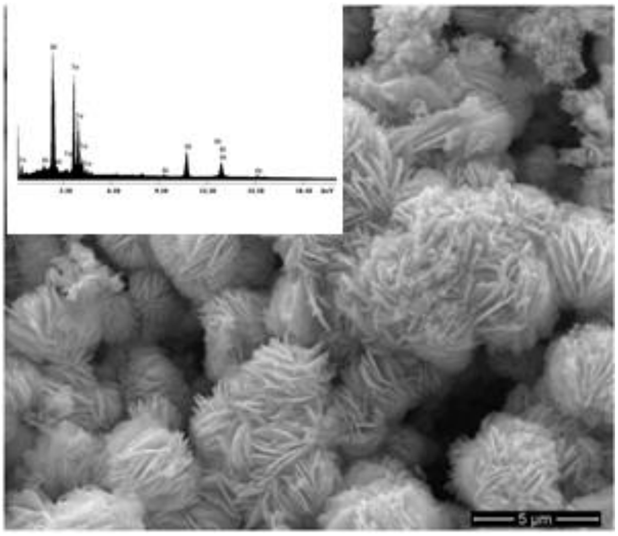

Fig. 3. SEM morphology for Bi_2Te_3 synthesized by ultrasonically assisted hydrothermal method at 11 pH; Inset: EDX spectra for elemental analysis.

3.3. AFM results

Fig. 4 shows the AFM images of surface morphology for S1 and S2. The AFM studies revealed non uniform surface for both samples. The average grain size for Bi_2Te_3 results from the analysis of AFM image with Scion Image and fitted with TableCurve software have the maximum at 31 nm for S1 and at 38 nm for S2 in good agreement with dimension results from the XRD pattern. The dimensional distribution function is LogNormal.

The roughness of the bismuth telluride can be quantitatively identified by the root mean-squared roughness (rms) (R_{rms}). Roughness is given by the standard deviation of the data from the AFM image, and determined using the standard definition:

$$R_{rms} = \mathrm{sqrt}\left(\sum_{n=1}^{N}\left(z_n - \bar{z}\right)^2 / N - 1\right).$$

Where z_n represents the height of the n-th data, $\bar{z}$ is equal to the mean height of Z_n in AFM topography, and N is the number of the data. For area 1.25 m^2 the average roughness is about 2.3 nm for S1 and about 2.6 nm for S2.

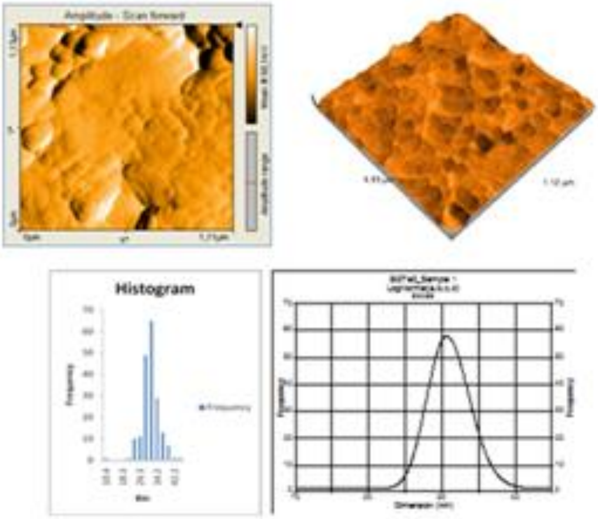

Fig.4. AFM image with scan area of 1.11 x 1.13 μm; histogram and particle size for Bi_2Te_3 synthesized by ultrasonically assisted hydrothermal method 8.5 pH.

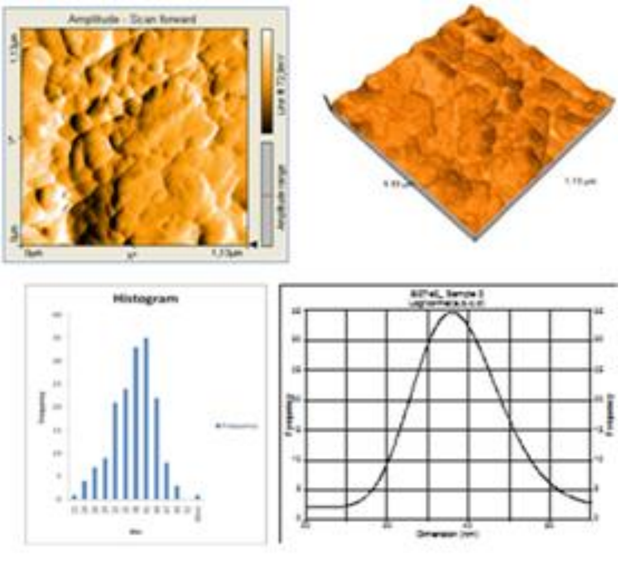

Fig. 5. AFM image with scan area of 1.11 x 1.13 μm; histogram and particle size for Bi_2Te_3 synthesized by ultrasonically assisted hydrothermal method at 11 pH.

4. Conclusions

Materials based on bismuth have been successfully synthesized through assisted hydrothermal method at different pH values. It was found that hydrothermal processing result in formation of low dimensional dispersion of Bi_2Te_3 nanostructures with desirable form and size and high degree of crystallinity.

The SEM analysis shows that the particles are flake shaped and strongly agglomerated. The EDAX analysis confirms the 2/3 ratio of the constituent atoms.

XRD pattern shows that the particles are crystallized in a single phase, the crystallite sizes being 30 nm (S1) and 40 nm (S2).

The average grain size for Bi_2Te_3 results from the analysis of AFM is 31 nm for S1 and at 38 nm for S2, both dimensional dispersion with LogNormal distribution.

Acknowledgements

This work is supported by the strategic grant POSDRU ID77265 (2010), co-financed by the European Social Fund – Investing in People, within the Sectoral Operational ProgrammeHuman Resources Development 2007-2013.

The authors thanks to the X-ray Diffraction and Electronic and Optical Microscopy Laboratories from the Characterization Department of National Institute for Research and Development in Electrochemistry and Condensed Matter, Timisoara for the characterization results.

References

[1] F. J. DiSalvo: Science **285**, 703 (1999).
[2] B. S. Sales: Science **295**, 1248 (2002).
[3] A. I. Hochbaum, et al. Enhanced thermoelectric performance of rough silicon nanowires. Nature **451**, 163 (2008).
[4] C. Kaito, Y. Saito, K. Fujita, J. Cryst. Growth 94, 967 (1989).
[5] F. D. Rosi, B. Ables, R. V. Jensen, J. Phys. Chem. Solids **10**, 191 (1959).
[6] M. S. Sander, A.L. Prieto, R. Gronsky, T. Sands, A. M. Stacy: Adv. Mater. **14**, (2002).
[7] M. Mart´ın-Gonz´alez, A. L. Prieto, R. Gronsky, T. Sands, A. M. Stacy: Adv. Mater. **15**, 665 (2003).
[8] R. Venkatasubramanian, E. Siivola, T. Colpitts, B. O'Quinn: Nature **413**, 597 (2001).
[9] T. C. Harman, P. J. Taylor, M. P. Walsh, B. E. LaForge: Science **297**, 2229 (2002).
[10] S. H. Yu, J. Yang, Y. S. Wu, Z. H. Han, J. Lu, Y. Xie, Y. T. Qian: J. Mater. Chem. **8**, 1949 (1998).
[11] Y. Deng, X. S. Zhou, G. D. Wei, J. Liu, C.W. Nan, S. J. Zhao: J. Phys. Chem. Solids **63**, 2119 (2002).
[12] M. A. Meitl, T. M. Dellinger, P. V. Braun: Adv. Funct. Mater. **13**, 795 (2003).
[13] Y. Deng, G. D. Wei, C.W. Nan: Chem. Phys. Lett. **368**, 639 (2003).
[14] Y. Deng, C. W. Nan, G. D. Wei, L. Guo, Y. H. Lin: Chem. Phys. Lett. **374**, 410 (2003).
[15] X. B. Zhao, Y. H. Zhang, X. H. Ji: Inorg. Chem. Comm. **7**, 386 (2004).
[16] X. B. Zhao, X. H. Ji, Y. H. Zhang, B. H. Lu: J. Alloys Compd. **368**, 349 (2004).
[17] X. B. Zhao, X. H. Ji, Y. H. Zhang, G. S. Cao, J. P. Tu, Appl. Phys. A **80**, 1567 (2005).
[18] R. Venkatasubramanian, T. Colpitts, E. Watko, M. Lamvik, N. El-Masry, J. Crystal Growth **170**, 817 (1997).
[19] A. Giani, F. Pascal-Delannoy, A. Foucaran, A. Boyer, M. Gschwind, P. Ancey, Thin Solid Films **303**, 1 (1997).
[20] A. Giani, A. Boulouz, F. Pascal-Delannoy, A. Foucaran, A. Boyer, Thin Solid Films **315**, 99 (1998).
[21] RO, CBI, D 2009 A00436/12.06.2009.
[22] P. Jeevanandam, Y. Diamant, M. Motiei, A. Gedanken, Phys. Chem. Chem. Phys. **3**, 4107 (2001).
[23] P. Cintas, J.-L. Luche, Green Chem. **1**(3), 115 (1999).
[24] A. Gedanken, Ultrason. Sonochem. **11**, 47 (2004).
[25] L. C. Hagenson, L. K. Doraiswamy, Chem. Eng. Sci. **53**, 131 (1997).
[26] A. Benhacene, P. Labbe, C. Petrier, G. Reverdy, New J. Chem. **19**, 989 (1995).

---

*Corresponding author: psfirloaga@yahoo.com